Cerebral cortex maldevelopment in syndromic craniosynostosis

ALEXANDER T WILSON[1,2] | BIANCA K DEN OTTELANDER[1] | MARIE-LISE C VAN VEELEN[3] | MARJOLEIN HG DREMMEN[4] | JOHN A PERSING[2] | HENRI A VROOMAN[4] | IRENE MJ MATHIJSSEN[1] | ROBERT C TASKER[5]

1 Department of Plastic and Reconstructive and Hand Surgery, Erasmus University Medical Center, Rotterdam, the Netherlands. **2** Section of Plastic Surgery, Yale School of Medicine, New Haven, CT, USA. **3** Department of Neurosurgery, Erasmus University Medical Center, Rotterdam; **4** Department of Radiology and Nuclear Medicine, Erasmus University Medical Center, Rotterdam, the Netherlands. **5** Department of Anesthesiology, Critical Care and Pain Medicine, Harvard Medical School, Boston Children's Hospital, Boston, MA, USA.

Correspondence to Alexander T Wilson, Department of Plastic and Reconstructive and Hand Surgery, Erasmus University Medical Center, Dr Molewaterplein 40, 3015 Rotterdam, the Netherlands. E-mail: a.wilson@erasmusmc.nl

PUBLICATION DATA
Accepted for publication 2nd June 2021.
Published online 15th July 2021.

ABBREVIATIONS

CSA	Cortical surface area
FGFR	Fibroblast growth factor receptor
ICV	Intracranial volume

AIM To assess the relationship of surface area of the cerebral cortex to intracranial volume (ICV) in syndromic craniosynostosis.

METHOD Records of 140 patients (64 males, 76 females; mean age 8y 6mo [SD 5y 6mo], range 1y 2mo–24y 2mo) with syndromic craniosynostosis were reviewed to include clinical and imaging data. Two hundred and three total magnetic resonance imaging (MRI) scans were evaluated in this study (148 patients with fibroblast growth factor receptor [*FGFR*], 19 patients with *TWIST1*, and 36 controls). MRIs were processed via FreeSurfer pipeline to determine total ICV and cortical surface area (CSA). Scaling coefficients were calculated from log-transformed data via mixed regression to account for multiple measurements, sex, syndrome, and age. Educational outcomes were reported by syndrome.

RESULTS Mean ICV was greater in patients with *FGFR* (1519cm^3, SD 269cm^3, p=0.016) than in patients with *TWIST1* (1304cm^3, SD 145cm^3) or controls (1405cm^3, SD 158cm^3). CSA was related to ICV by a scaling law with an exponent of 0.68 (95% confidence interval [CI] 0.61–0.76) in patients with *FGFR* compared to 0.81 (95% CI 0.50–1.12) in patients with *TWIST1* and 0.77 (95% CI 0.61–0.93) in controls. Lobar analysis revealed reduced scaling in the parietal (0.50, 95% CI 0.42–0.59) and occipital (0.67, 95% CI 0.54–0.80) lobes of patients with *FGFR* compared with controls. Modified learning environments were needed more often in patients with *FGFR*.

INTERPRETATION Despite adequate ICV in *FGFR*-mediated craniosynostosis, CSA development is reduced, indicating maldevelopment, particularly in parietal and occipital lobes. Modified education is also more common in patients with *FGFR*.

Craniosynostosis is a congenital disorder characterized by premature fusion of calvarial sutures resulting in cranial shape deformity specific to the sutures involved. This shape is governed by Virchow's law which states that growth is enhanced parallel to affected sutures and is arrested orthogonally. Invariably, every pattern of true cranial growth restriction poses a risk to the developing brain and is treated accordingly with various surgical interventions. Multiple suture involvement often occurs in syndromic variants of the disease attributable to mutations in fibroblast growth factor receptor (*FGFR*; Apert, Crouzon–Pfeiffer, and Muenke syndromes) and *TWIST1* (Saethre-Chotzen syndrome) genes which play important roles in cortical and mesodermal development respectively.[1,2] Thus, cranial growth restriction as well as genetic mutation may play a role in neurodevelopmental outcomes in syndromic craniosynostosis.

Allometry can be broadly defined as the relative change in proportion of one attribute compared to another during organismal growth. In general, human brain growth exhibits a power law scaling relationship between surface area and volume as overall brain size increases, with larger brains showing disproportionally greater surface area than smaller ones.[3–6] This is achieved through primary, secondary, and tertiary cortical folding driven by grey matter volume expansion and white matter tension in the second and third trimesters.[7,8] Disruption of this critical process, through preterm birth or intrauterine growth restriction, results in reduced surface area to volume scaling and predictable impairment in neurobehavioral development.[9]

Because of the increased frequency of neurodevelopmental issues in syndromic craniosynostosis and the pathognomonic cranial growth restriction characteristic of the disease, we wondered if there might exist a morphometric neural substrate for the developmental pathology in these cases. Thus, our primary aim was to evaluate the effect of syndromic craniosynostosis diagnosis on intracranial volume (ICV), while controlling for age and sex. A secondary

 DOI: 10.1111/dmcn.14984

aim was to evaluate the scaling relationship between ICV and cortical surface area (CSA). Finally, we carried out exploratory analyses of this relationship in distinct cortical lobes.

What this paper adds

- Cerebral cortex development in fibroblast growth factor receptor [*FGFR*]-mediated craniosynostosis is marked by reduced surface area relative to intracranial volume.
- This is particularly apparent in the parietal and occipital lobes.
- Scholastic outcomes are worse in *FGFR*-mediated craniosynostosis syndromes compared to patients with *TWIST1* or controls.

METHOD

Participants

The Institution Research Ethics Board at Erasmus University Medical Center, Rotterdam, the Netherlands approved this study (MEC-2014-461), which is part of ongoing work at the Dutch Craniofacial Center involving protocolized care, brain imaging, clinical assessment, and data summary and evaluation. Medical records of all patients with syndromic (Apert, Crouzon–Pfeiffer, Muenke, and Saethre-Chotzen syndromes) craniosynostosis treated at our center from 2008 to 2018 were reviewed and demographic data were collected. Patients were included if they had undergone 3D T1-weighted cranial magnetic resonance imaging (MRI) with fast spoiled gradient echo which could be successfully processed via FreeSurfer (version 6.0, https://surfer.nmr.mgh.harvard.edu; Athinoula A Martinos Center for Biomedical Imaging, Massachusetts General Hospital, Boston MA, USA) 'auto-recon' pipeline. Patients with imaging not suitable for processing were excluded from further analysis. All available imaging data were utilized including multiple MRIs of the same patient at different time points. All patients with syndromic craniosynostosis underwent cranial vault expansion surgery before any MRIs included in this study. Control patients of a similar age and sex with appropriate MRI sequences were also identified and included for analysis. Indications for imaging included headache, head trauma, single seizure episode, early menstruation, hypoglycemia, and heat intolerance. Indications for imaging were reviewed by a pediatric neurosurgeon and deemed suitable for comparison to our cohort of patients with syndromic craniosynostosis.

MRI acquisition

All MRI scans were performed on a 1.5T scanner (GE Healthcare, MR Signa Excite HD, Little Chalfont, UK) with the imaging protocol including a 3D fast spoiled gradient echo T1-weighted magnetic resonance sequence. Imaging parameters for patients with craniosynostosis were the following: 2mm slice thickness, no slice gap; field of view 22.4cm; matrix size 224 × 224; in plane resolution of 1mm; echo time 3.1ms, and repetition time 9.9ms.

Cortical volume, CSA, and ICV

MRI dicom files were exported and converted to neuroimaging informatics technology initiative file format on a computer cluster with Scientific Linux as the operating system and preloaded FreeSurfer software. All cortical volume, CSA, and ICV values were obtained from FreeSurfer software modules which have previously been validated and described in detail.[10–12] Each MRI underwent processing via the 'auto-recon-all' pipeline which generates pial and white matter surfaces and allows for accurate estimation of cortical volume, surface area, and ICV values. After initial processing, all surfaces generated by FreeSurfer were inspected visually to ensure accuracy. No manual editing or alteration of the generated surfaces was performed. Lobar cortical volume and surface area estimates were generated via the '--lobes' argument within the 'mris_annotation2label' command. A total of six lobes (frontal, temporal, parietal, occipital, cingulate, insula) in each hemisphere are included in the FreeSurfer parcellation. Left and right hemispheric outputs were summed to generate whole lobe values for statistical analysis. Total ICV was exported from FreeSurfer as 'eTIV' via the 'mri_segstats' command. These techniques have previously been applied with success in the population with craniosynostosis.[13,14]

Scaling coefficient

Objects of invariant shape but variable size demonstrate a geometric scaling relationship which can be expressed as: $s=kv^{\alpha}$ (where s=surface area, v=volume, k=constant, and $\alpha=2/3$ is a scaling exponent).[5] The coefficient α can be obtained by log transformation yielding: $log(s)=\alpha\ log(v)+log(k)$

Therefore, plotting $log(v)$ and $log(s)$ by linear regression, the slope of the line is equal to α with the intercept equal to $log(k)$. Deviations from $\alpha=2/3$ would then provide information regarding accelerated ($\alpha>2/3$) or reduced ($\alpha<2/3$) surface area to volume scaling than otherwise expected from geometric principles. This technique has previously been demonstrated as a measure for cortical development sensitive to environmental effects and has been correlated to neurocognitive outcomes in neonates.[5] An additional advantage is that the resulting exponent is unitless and may be compared across cohorts.

Education level

In an attempt to evaluate long-term functional outcome, data regarding educational placement were gathered from medical chart review in readily available cases. Educational placement in the Netherlands has varying levels of organization aimed at preparation for individuals pursuing a variety of career paths. Placement is made by both examination and recommendation by primary school teachers. For simplification, patients were organized into three distinct groups: (1) those requiring modified instruction or expanded services to complete their primary/secondary schooling; (2) those completing standard coursework without impairment; (3) those completing coursework in preparation for university study. For those in group 1, additional data regarding the nature of services provided were gathered and the following subgroups used: (1a)

visual impairment; (1b) hearing or speech impairment; (1c) motor or intellectual disability: (1d) psychological or behavioral problems; (1e) mild learning problems.

Statistical analysis

All data were imported into R statistical software (version 3.6.1, R Foundation for Statistical Computing, Vienna, Austria) for analysis. To assess intergroup differences in ICV, a linear mixed effects regression ('nlme' package) was used while controlling for sex, age, and repeated measurements within the same participant (fit by maximum likelihood). Independent variables included age at the time of MRI, sex, and genetic group. The dependent variable was ICV. The only random effect term included was participant identity which served as an index for each MRI included. Although repeated measurements were not available for every participant, the 'lme' function in R eliminates complete-case bias while incorporating all available data.[15] Model assumptions were also checked. Linearity was assessed graphically ('lattice' package). Normality of residuals was verified via Q–Q plot ('stats' package). Similarly, log-transformed mixed regression models were used for evaluating CSA to ICV scaling relationships by genetic status. Patients were organized into control, *TWIST1*, and *FGFR* groups initially and later split into specific syndromes for subgroup analysis. Exploratory analysis was performed to evaluate potential regional differences in CSA to ICV scaling by lobe via linear mixed regression. Last, frequency tables were generated by syndrome for educational placement data. For the primary aim (global model), coefficents, 95% confidence intervals (CIs), and *p*-values are reported. For the secondary aim and exploratory analysis, coefficients and 95% CIs are reported.

RESULTS

In total, 203 MRI scans from 140 participants (64 males, 76 females; mean age 8y 6mo [SD 5y 6mo], range 1y 2mo–24y 2mo) were included for analysis in this study. Four outlier MRIs were excluded with ICV less than 1000cm^3 including one control and three patients with Saethre-Chotzen syndrome which appeared to negatively skew ICV results in the *TWIST1* group. Before removal of outliers, mean *TWIST1* ICV was 1250cm^3 (SD 195cm^3) compared to final mean *TWIST1* ICV of 1304cm^3 (SD 145cm^3). Mean control ICV was 1393cm^3 (SD 170cm^3) compared to final control mean ICV of 1405cm^3 (SD 158cm^3) after outlier exclusion. In the final data set there were 37 cases of Apert syndrome, 86 Crouzon–Pfeiffer syndrome, 25 Muenke syndrome, 19 Saethre-Chotzen syndrome, and 36 typically developing controls. A summary of the final data set is shown in Table 1. Mean age at the time of MRI was 9 years (SD 5y 3mo). For the primary aim, mean ICV was 1519cm^3 (SD 270cm^3) in patients with *FGFR*, which was greater than that observed in controls (p=0.016). In patients with *TWIST1* mutations, ICV was no different from controls (mean=1251cm^3, p=0.080). As expected, age was positively associated with ICV (p<0.001) and female sex was negatively correlated (p<0.001). Complete results of the primary model are shown in Table 2.

Table 1: Participant characteristics from MRIs shown grouped by mutation status

	Control	*FGFR*	*TWIST1*
Mean age (SD), y:mo	9:3 (5:5)	8:9 (4:10)	10:7 (7:9)
Female, *n* (%)	21 (58.3)	74 (50)	13 (68.4)
ICV (cm^3)	1405 SD 158	1519 SD 270	1304 SD 145
CSA (cm^2)	1744 SD 176	1945 SD 281	1764 SD 192
MRI, *n*	36	148	19
Participants, *n*	36	89	15

For age, intracranial volume (ICV) and cortical surface area (CSA) mean (SD) are reported. Numerical values are calculated from total magnetic resonance imaging (MRI) scans. *FGFR*, fibroblast growth factor receptor.

For the secondary aim, CSA to ICV scaling coefficients were obtained by log transformation. Genetic groupings were maintained for analysis but further subdivided into specific syndromic diagnosis (Fig. 1). Patients with *FGFR* collectively yielded a scaling coefficient α_{FGFR}=0.68 (95% CI 0.61–0.76) with the syndromic subgroup coefficients as α_{apert}=0.53 (95% CI 0.38–0.69), $\alpha_{crouzon-pfeiffer}$=0.69 (95% CI 0.59–0.79), and α_{muenke}=0.56 (95% CI 0.38–0.74) compared to patients with *TWIST1*/Saethre-Chotzen syndrome $\alpha_{saethre-chotzen}$=0.81 (95% CI 0.50–1.12) and controls $\alpha_{control}$=0.77 (95% CI 061–0.93). Lobar analysis (shown in Table 3) revealed smaller scaling coefficients in the parietal lobes of both patients with *TWIST1* ($\alpha_{parietal}$=0.39, 95% CI –0.24 to 1.03) and patients with *FGFR* ($\alpha_{parietal}$=0.50, 95% CI 0.42–0.59) compared to controls ($\alpha_{parietal}$=0.71, 95% CI 0.50–0.93). The occipital lobes of patients with *FGFR* also demonstrated reduced CSA/ICV scaling ($\alpha_{occipital}$=0.67, 95% CI 0.54–0.80) compared to controls ($\alpha_{occipital}$=0.83, 95% CI 0.53–1.13). Brain surfaces of patients from each syndrome are shown in Figure 2.

Of the 104 patients with syndromic craniosynostosis included in the study, educational data were available in 103. Frequency tables for education level are shown in Table 4. All but one patient requiring modified education were from the *FGFR* group. The majority (74%) of patients with Apert syndrome required modified education, with six (26%) completing standard coursework without assistance. Of the patients requiring modified education, subgroup analysis revealed none were because of blindness/vision impairment, two (one Crouzon–Pfeiffer syndrome, one Muenke syndrome) were because of hearing impairment, 19 (10 Apert syndrome, eight Crouzon–Pfeiffer syndrome, one Muenke syndrome) were because of motor or intellectual disability, four (two Crouzon–Pfeiffer syndrome, two Muenke syndrome) were because of psychological or behavioral problems, and 11 (seven Apert syndrome, one Crouzon–Pfeiffer syndrome, two Muenke syndrome, one Saethre-Chotzen syndrome) had mild learning problems.

DISCUSSION

The purpose of this study was to evaluate neuromorphological development in syndromic craniosynostosis as it relates to cranial growth. Since ICV is a marker of cranial

Table 2: Linear mixed effects model evaluating differences in intracranial volume associated with *FGFR* and *TWIST1* mutations compared to controls

Predictors	Estimates	95% CI	*p*
Intercept	1338.72	1247.85–1429.59	**<0.001**
Age	17.20	12.26–22.13	**<0.001**
Females	−160.06	−229.11 to −91.01	**<0.001**
FGFR	101.27	20.15–182.38	**0.016**
TWIST1	−114.00	−240.14 to 12.14	0.080

Model is fit by maximum likelihood. Random effect intercept=188.77 and residual=89.10. CI, confidence interval; *FGFR*, fibroblast growth factor receptor.

growth and its expansion often the aim of surgical intervention, it serves as a useful metric in the population with syndromic craniosynostosis.[16,17] Our primary analysis revealed larger ICV values in patients with craniosynostosis with FGFR mutations compared to controls, but despite these larger volumes, a commensurate increase in cerebral CSA was not observed. Further analysis indicates that reduced scaling of CSA to ICV is most severe in the parietal and occipital lobes for patients with FGFR. Given the high rate of neuropsychiatric and developmental issues in this population, these findings may provide a morphometric neural substrate for such outcomes.[18]

Craniocerebral disproportion is a hallmark of craniosynostosis resulting from inadequate ICV for the developing brain. Targeted volume expansion through surgical intervention seeks to improve this and clinical measurements such as occipitofrontal circumference are even made as a proxy for ICV growth.[16,19–21] Previous data support our findings of elevated ICV in *FGFR*-mediated craniosynostosis, as larger volumes have been reported in patients with Apert, Muenke, and Crouzon–Pfeiffer syndromes compared with typically developing controls.[17,22–25] ICV data is limited regarding Muenke syndrome, but Rijken et al. have shown increased posterior fossa and cerebellar volumes in these patients.[26] Lastly, in a study by Breakey et al.,[17] ICV and head circumference were measured in a series of children with syndromic craniosynostosis and similar values in patients with Saethre-Chotzen syndrome and controls were observed, which also coincides with our current findings.

Despite larger ICV, patients with *FGFR* did not demonstrate typical CSA development. Growth of the cerebral cortex is primarily driven by an increase in CSA which scales disproportionally as brain size increases.[5] Disruptions to surface area maturation have been associated with various developmental pathologies common to the population with syndromic craniosynostosis including cognitive

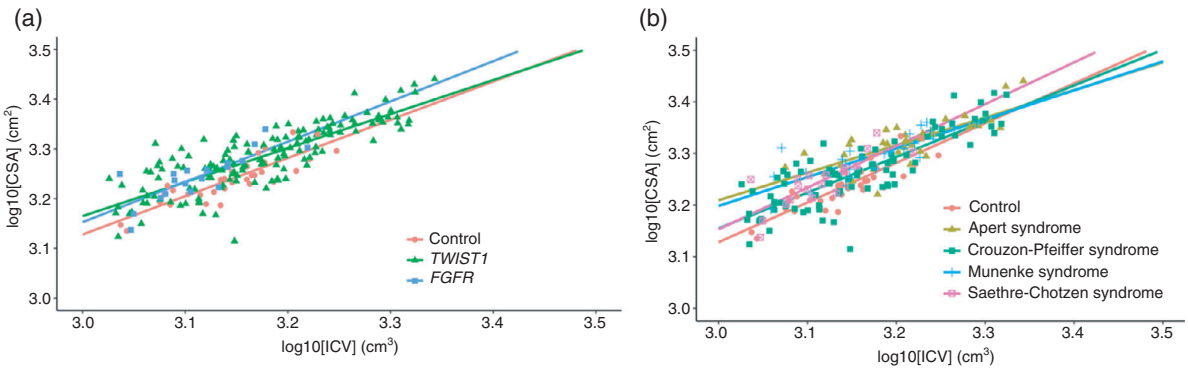

Figure 1: Cortical surface area plotted against intracranial volume (ICV) in log-log space for each genetic grouping as well as by syndrome. Slopes are equal to scaling coefficients. CSA, cortical surface area; *FGFR*, fibroblast growth factor receptor.

Table 3: Linear mixed regression models of log-transformed data for each lobe, organized by genetic status

	Control (*n*=36)			*FGFR* (*n*=148)			*TWIST* (*n*=19)		
	Slope	95% CI	Intercept	Slope	95% CI	Intercept	Slope	95% CI	Intercept
Frontal	0.76	0.56–0.95	2.07	0.73	0.62–0.84	2.16	0.81	0.33–1.30	1.91
Temporal	0.86	0.66–1.04	1.51	0.80	0.69–0.92	1.72	0.70	0.24–1.17	1.99
Parietal	0.71	0.50–0.93	2.10	0.50	0.42–0.59	2.79	0.39	–0.24 to 1.03	3.13
Occipital	0.83	0.53–1.13	1.42	0.67	0.54–0.80	1.94	1.18	0.71–1.65	0.37
Cingulate	0.94	0.66–1.22	0.56	0.79	0.61–0.96	1.06	1.11	0.69–1.53	0.07
Insula	0.87	0.61–1.13	0.61	0.75	0.60–0.90	1.00	0.98	0.46–1.50	0.28

$\log_{10}[CSA] = m \log_{10}[ICV] + b$. *m*=slope, 95% confidence interval (CI) for each slope given, *b*=intercept. Dependent variable is cortical surface area (CSA). Independent variable is intracranial volume (ICV). *FGFR*, fibroblast growth factor receptor.

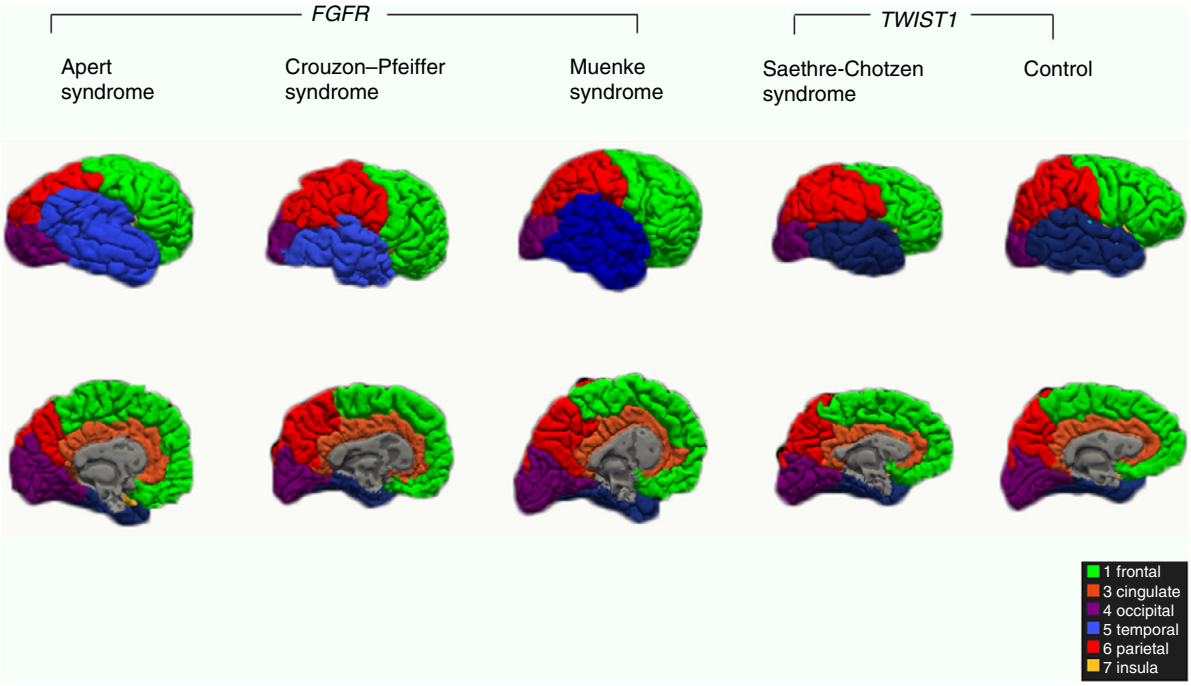

Figure 2: Brain surfaces with lobar parcellation shown for each syndrome and genetic grouping. *FGFR*, fibroblast growth factor receptor.

Table 4: Educational placement by genetic status/syndrome

	FGFR			*TWIST1*
	Apert syndrome	Crouzon–Pfeiffer syndrome	Muenke syndrome	Saethre-Chotzen syndrome
Group 1	17 (74)	12 (27)	6 (27)	1 (7)
Group 2	6 (26)	27 (61)	16 (73)	9 (64)
Group 3	0	5 (11)	0	4 (29)
Total	23	44	22	14

Data are *n* (%). Group 1 patients required special schooling or accommodation during their primary education years. Group 2 patients completed standard coursework at a regular school. Group 3 patients completed coursework in preparation for university study. *FGFR*, fibroblast growth factor receptor.

impairment and neurobehavioral disorders.[5,27,28] Regional analysis revealed that scaling was most drastically reduced in the parietal and occipital lobes for patients with *FGFR*. Although no reduction in global scaling coefficient was detected for patients with *TWIST1*, lobar analysis showed similar reductions in parietal lobe CSA to ICV scaling. Previous work by Skranes et al. demonstrated an association between reduced CSA in infants born preterm and reductions in IQ.[29] In that study, the parietal cortex was implicated in multiple measures of intelligence including working memory, processing speed, and perceptual organization. Occipital cortex development is important for visual processing ability which, if impaired, could manifest as a reading disability or otherwise be detrimental to scholastic achievement.[30–32] Interestingly, Raschle et al. showed that children with reading disability demonstrated reduced surface area in posterior regions of the brain without compensatory changes in the frontal lobe typical of adults with the disorder.[32] Lack of early surface area maturation in the brain may explain some developmental issues observed in these patients with syndromic craniosynostosis.

Although detailed neuropsychological data were unavailable in our cohort, evaluation of educational data showed that all patients requiring modified placement had an *FGFR*-mediated form of craniosynostosis. Further subgroup analysis showed that the majority of patients with Apert syndrome requiring modified education suffered from motor or intellectual disability, while psychological or behavioral issues were more common in patients with Muenke syndrome. Crouzon–Pfeiffer syndrome placement was highly variable and patients with Saethre-Chotzen syndrome all undertook normal or advanced coursework

which is congruent with our neuromorphometrical findings. Previous neuropsychological outcomes in the population with syndromic craniosynostosis show a similar pattern of intellectual disability in patients with Apert syndrome and higher prevalence of social or behavioral problems in patients with Muenke syndrome.[18]

The link between cortical maldevelopment and neuropsychological issues in syndromic craniosynostosis appears likely; however, the specific cause remains elusive. Because of different genetic mechanisms among the various syndromes, inborn errors of cortical folding or maturation may exist and may vary significantly among syndrome and subtype. For example, *FGFR* genes are critical in cortical development processes including neuronal migration and stabilization of dentritic patterning and *TWIST1* is involved in cranial mesodermal development.[33–35] Other factors may also influence cortical development including craniocerebral disproportion, intracranial hypertension, surgical intervention, and associated anesthesia burden. Future studies with consistent serial imaging and detailed neuropsychological assessment may provide greater insight regarding specific causes of the cortical maldevelopment described here.

When interpreting the findings of this study several limitations should be considered. First, serial MRI scans were not available for each patient limiting the utility of longitudinal inferences regarding cortical maturation. For those patients in whom multiple MRIs were available, all scans were included via mixed effects regression modeling to fully utilize available data. We also considered the possibility of selection bias in both the population with syndromic craniosynostosis and controls. All patients with syndromic craniosynostosis are systematically evaluated by MRI as a part of standardized protocol and control patients were carefully selected based on indication so as to remove any with pathology pertinent to our analysis. Lastly, one control and three patients with Saethre-Chotzen syndrome were excluded as outliers with significantly reduced ICVs that appeared to negatively skew ICV results in the *TWIST1* group. Before the removal of outliers, mean *TWIST1* ICV was 1250cm^3 compared to final mean *TWIST1* ICV of 1304cm^3 and mean control ICV was 1393cm^3 compared to final control mean ICV of 1405cm^3. Regarding development, two-thirds of the patients with Saethre-Chotzen syndrome excluded based on outlier position had normal education outcomes so it is unlikely that we introduced a bias.

In this study we documented the paradoxical increase in ICV from cranial growth restriction in *FGFR*-mediated syndromic craniosynostosis. We also established that despite adequate volume, cerebral cortex development remains atypical in this patient population. Specifically, we identified reduced scaling of CSA to ICV in the parietal and occipital lobes and observed corresponding deficits in scholastic achievement primarily in Apert syndrome. Explanations for these findings include genetic influences on cortex folding, physical constraints on the expanding cerebral cortex, intracranial hypertension, and sequelae from surgical intervention. Further study is needed to elucidate precise mechanisms of cortical development in craniosynostosis and their link to neuropsychiatric outcomes. Clinically, identification of in vivo biomarkers sensitive to treatment variation and functional outcomes would help in optimizing care protocols for patients with craniosynostosis. With further study, CSA/ICV scaling may prove useful as such.

ACKNOWLEDGEMENTS

The authors have stated they had no interests that might be perceived as posing a conflict or bias.

DATA AVAILABILITY STATEMENT

Author elects to not share data.

REFERENCES

1. Stevens HE, Smith KM, Maragnoli ME, et al. Fgfr2 is required for the development of the medial prefrontal cortex and its connections with limbic circuits. *J Neurosci* 2010; **30**: 5590–602.
2. Qin Q, Xu Y, He T, Qin C, Xu J. Normal and disease-related biological functions of Twist1 and underlying molecular mechanisms. *Cell Res* 2012; **22**: 90–106.
3. Hofman MA. Size and shape of the cerebral cortex in mammals. I. The cortical surface. *Brain Behav Evol* 1985; **27**: 28–40.
4. Hofman MA. On the evolution and geometry of the brain in mammals. *Prog Neurobiol* 1989; **32**: 137–58.
5. Kapellou O, Counsell SJ, Kennea N, et al. Abnormal cortical development after premature birth shown by altered allometric scaling of brain growth. *PLoS Med* 2006; **3**: e265.
6. Hofman MA. Design principles of the human brain: an evolutionary perspective. *Prog Brain Res* 2012; **195**: 373–90.
7. Garcia KE, Robinson EC, Alexopoulos D, et al. Dynamic patterns of cortical expansion during folding of the preterm human brain. *Proc Natl Acad Sci USA* 2018; **115**: 3156–61.
8. Dubois J, Benders M, Cachia A, et al. Mapping the early cortical folding process in the preterm newborn brain. *Cereb Cortex* 2007; **18**: 1444–54.
9. Dubois J, Benders M, Borradori-Tolsa C, et al. Primary cortical folding in the human newborn: an early marker of later functional development. *Brain* 2008; **131**: 2028–41.
10. Dale AM, Fischl B, Sereno MI. Cortical surface-based analysis. I. Segmentation and surface reconstruction. *Neuroimage* 1999; **9**: 179–94.
11. Fischl B, Dale AM. Measuring the thickness of the human cerebral cortex from magnetic resonance images. *Proc Natl Acad Sci USA* 2000; **97**: 11050–5.
12. Fischl B, Sereno MI, Dale AM. Cortical surface-based analysis. II: inflation, flattening, and a surface-based coordinate system. *Neuroimage* 1999; **9**: 195–207.
13. Wilson AT, de Planque CA, Yang SS, et al. Cortical thickness in Crouzon-Pfeiffer syndrome: findings in relation to primary cranial vault expansion. *Plast Reconstr Surg Glob Open* 2020; **8**: e3204.
14. Wilson AT, Den Ottelander BK, De Goederen R, et al. Intracranial hypertension and cortical thickness in syndromic craniosynostosis. *Dev Med Child Neurol* 2020; **62**: 799–805.
15. Ibrahim JG, Molenberghs G. Missing data methods in longitudinal studies: a review. *Test (Madr)* 2009; **18**: 1–43.

16. Spruijt B, Rijken BFM, den Ottelander BK, et al. First vault expansion in Apert and Crouzon-Pfeiffer syndromes: front or back? *Plast Reconstr Surg* 2016; **137**: 112e–21e.
17. Breakey RWF, Knoops PGM, Borghi A, et al. Intracranial volume and head circumference in children with unoperated syndromic craniosynostosis. *Plast Reconstr Surg* 2018; **142**: 708e–17e.
18. Maliepaard M, Mathijssen IM, Oosterlaan J, Okkerse JM. Intellectual, behavioral, and emotional functioning in children with syndromic craniosynostosis. *Pediatrics* 2014; **133**: e1608–15.
19. Rijken BF, den Ottelander BK, van Veelen ML, Lequin MH, Mathijssen IM. The occipitofrontal circumference: reliable prediction of the intracranial volume in children with syndromic and complex craniosynostosis. *Neurosurg Focus* 2015; **38**: E9.
20. Hashmi A, Cahill GL, Zaldana M, et al. Can head circumference be used as a proxy for intracranial volume in patients with craniosynostosis? *Ann Plast Surg* 2019; **82**(Suppl. 4): S295–300.
21. Serlo WS, Ylikontiola LP, Lähdesluoma N, et al. Posterior cranial vault distraction osteogenesis in craniosynostosis: estimated increases in intracranial volume. *Childs Nerv Syst* 2011; **27**: 627–33.
22. Sgouros S, Hockley AD, Goldin JH, Wake MJ, Natarajan K. Intracranial volume change in craniosynostosis. *J Neurosurg* 1999; **91**: 617–25.
23. Posnick JC, Armstrong D, Bite U. Crouzon and Apert syndromes: intracranial volume measurements before and after cranio-orbital reshaping in childhood. *Plast Reconstr Surg* 1995; **96**: 539–48.
24. Muenke M, Gripp KW, McDonald-McGinn DM, et al. A unique point mutation in the fibroblast growth factor receptor 3 gene (FGFR3) defines a new craniosynostosis syndrome. *Am J Hum Genet* 1997; **60**: 555–64.
25. Moloney DM, Wall SA, Ashworth GJ, et al. Prevalence of Pro250Arg mutation of fibroblast growth factor receptor 3 in coronal craniosynostosis. *Lancet* 1997; **349**: 1059–62.
26. Rijken BFM, Lequin MH, van der Lijn F, et al. The role of the posterior fossa in developing Chiari I malformation in children with craniosynostosis syndromes. *J Craniomaxillofac Surg* 2015; **43**: 813–9.
27. Sarkar S, Daly E, Feng Y, et al. Reduced cortical surface area in adolescents with conduct disorder. *Eur Child Adolesc Psychiatry* 2015; **24**: 909–17.
28. Batty MJ, Palaniyappan L, Scerif G, et al. Morphological abnormalities in prefrontal surface area and thalamic volume in attention deficit/hyperactivity disorder. *Psychiatry Res* 2015; **233**: 225–32.
29. Skranes J, Løhaugen GC, Martinussen M, Håberg A, Brubakk AM, Dale AM. Cortical surface area and IQ in very-low-birth-weight (VLBW) young adults. *Cortex* 2013; **49**: 2264–71.
30. Kaiser D, Cichy RM. Typical visual-field locations enhance processing in object-selective channels of human occipital cortex. *J Neurophysiol* 2018; **120**: 848–53.
31. Pleisch G, Karipidis II, Brauchli C, et al. Emerging neural specialization of the ventral occipitotemporal cortex to characters through phonological association learning in preschool children. *Neuroimage* 2019; **189**: 813–31.
32. Raschle NM, Zuk J, Gaab N. Functional characteristics of developmental dyslexia in left-hemispheric posterior brain regions predate reading onset. *Proc Natl Acad Sci USA* 2012; **109**: 2156–61.
33. Huang JY, Lynn Miskus M, Lu HC. FGF-FGFR mediates the activity-dependent dendritogenesis of layer IV neurons during barrel formation. *J Neurosci* 2017; **37**: 12094–105.
34. Huang J-Y, Krebs BB, Miskus ML, et al. Enhanced FGFR3 activity in postmitotic principal neurons during brain development results in cortical dysplasia and axonal tract abnormality. *Sci Rep* 2020; **10**: 18508.
35. Bildsoe H, Fan X, Wilkie EE, et al. Transcriptional targets of TWIST1 in the cranial mesoderm regulate cell-matrix interactions and mesenchyme maintenance. *Dev Biol* 2016; **418**: 189–203.